Chinese Chemical Letters 36 (2025) 109770

Contents lists available at ScienceDirect

Chinese Chemical Letters

journal homepage: www.elsevier.com/locate/cclet

The counterintuitive aromaticity of bent metallabenzenes: A theoretical exploration

Quan Zhou[a,b], Xiao-Min Chen[a,c], Xujie Qin[a,b], Zhe-Ning Chen[a,b,d,*], Jun Chen[a,b,d,*], Wei Zhuang[a,b,d,*]

[a] State Key Laboratory of Structural Chemistry, Fujian Institute of Research on the Structure of Matter, Chinese Academy of Sciences, Fuzhou 350002, China
[b] University of Chinese Academy of Sciences, Beijing 100049, China
[c] College of Chemistry, Fuzhou University, Fuzhou 350108, China
[d] Fujian Provincial Key Laboratory of Theoretical and Computational Chemistry, Xiamen 361005, China

ARTICLE INFO

Article history:
Received 31 December 2023
Revised 18 February 2024
Accepted 14 March 2024
Available online 15 March 2024

Keywords:
Metallabenzenes
Metalla-aromaticity
σ-Control
NICS
Functional materials

ABSTRACT

Metallabenzenes, a type of aromatic compound that includes metal atoms, have opened up new avenues for creating materials with unique properties. A distinctive feature of metallabenzenes is the significant deviation of their metal atoms from the planar configuration of the C5 ring, a phenomenon that paradoxically enhances their aromatic character. In this investigation, we propose that this counterintuitive increase in aromaticity upon geometric distortion is governed by the interactions of frontier orbitals in the σ-space. This insight not only corroborates the previously suggested role of σ-space orbitals in inducing geometric non-planarity in metallabenzenes but also underscores their pivotal contribution to the compounds' enhanced aromaticity. As a result, this work broadens the scope of the σ-control mechanism, highlighting its usefulness for the rational design of functional metalla-aromatic materials.

Metalla-aromatics [1–7], conceptualized as aromatic ring systems incorporating a metal atom, have attracted significant attention due to their unique properties, positioning them as viable candidates for developing novel functional materials. Metallabenzenes [8–13], serving as the quintessential examples of metalla-aromatics, were first theoretically proposed by Hoffmann [14] and colleagues. The aromatic nature of metallabenzenes remains a subject of ongoing debate. Hoffmann *et al.* posited that metallabenzenes can be described as a $3\pi-6e$ system, conforming to Hückel's 4n+2 rule and classifying them as aromatic compounds. They argued that metallabenzenes should be isolobal with benzene and thus adhere to Hückel's 4n+2 rule. In contrast, Schleyer *et al.* [8] contended that metallabenzenes should be viewed as a $4\pi-8e$ system while acknowledging their aromatic character, albeit weaker than benzene. Subsequent research [15,16] has suggested that the π-space of metallabenzenes is more accurately described as a $5\pi-10e$ system, which also fulfills Hückel's aromaticity criterion. Consequently, metallabenzenes are broadly accepted as aromatic compounds, albeit with varying degrees of aromaticity.

In addition to their aromatic character, metallabenzenes exhibit another intriguing structural feature [17–20]: A pronounced deviation of the metal atom from the plane of the C5 ring, as corroborated by numerous entries in crystallographic databases. This non-planarity is counterintuitive, given that conjugation typically necessitates a planar arrangement.

Lin [20] and colleagues posited that metallabenzenes, owing to the inclusion of a transition metal fragment, should be conceptualized as a $4\pi-8e$ system featuring three bonding (π_1, π_2, and π_3) and one antibonding (π_4) orbitals. They further asserted that the bent geometry of metallabenzenes is predominantly governed by the π_4 orbital, which serves as the highest occupied molecular orbital (HOMO). Contrary to this perspective, our previous study [21–23] suggested that the non-planarity in metallabenzenes is minimally influenced by the π orbitals. We proposed that the primary driving force behind the observed geometric distortion is the antibonding interaction between an occupied metal d orbital and the σ orbitals of the C5 ring. We termed this the σ-control mechanism, providing a compelling rationale for the non-planar configuration of metallabenzenes.

Metallabenzenes are generally categorized as aromatic compounds and predominantly adopt near-planar configurations. Con-

* Corresponding authors at: State Key Laboratory of Structural Chemistry, Fujian Institute of Research on the Structure of Matter, Chinese Academy of Sciences, Fuzhou 350002, China.
E-mail addresses: znchen@fjirsm.ac.cn (Z.-N. Chen), chenjun@fjirsm.ac.cn (J. Chen), wzhuang@fjirsm.ac.cn (W. Zhuang).

https://doi.org/10.1016/j.cclet.2024.109770
1001-8417/

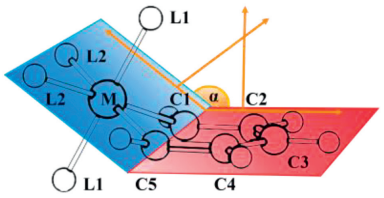

Scheme 1. The definition of dihedral angle α.

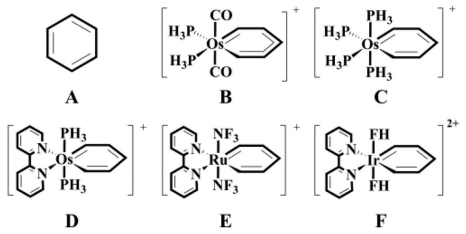

Scheme 2. Some illustrative bent metallabenzene complexes (B–F) and benzene (A).

sequently, the influence of geometric deviations on their physicochemical properties has yet to be largely overlooked. Our prior research proposed a σ-control mechanism to elucidate the electronic factors driving the observed geometric distortions in metallabenzenes [21]. However, the implications of such distortions on the aromaticity of these unique compounds, particularly the unanticipated enhancement in aromaticity upon bending, remain enigmatic. In the current investigation, we establish that, unlike traditional Hückel aromatic systems such as benzene, the electronic attributes of metallabenzenes are not predominantly governed by the π orbitals. Our data unambiguously reveal that the π orbitals alone cannot account for the increased aromaticity in bent metallabenzenes. Instead, we ascertain that the σ orbitals play a decisive role in the geometric deformations and the concomitant enhancement of aromatic properties in metallabenzenes, thereby diverging markedly from their benzene counterparts. These findings accentuate the distinct behavior between conventional benzene-like aromatics and metalla-aromatics, highlighting the critical role of the σ orbitals in the latter.

Continuing our prior work, we employ the dihedral angle α $=\angle$C2−C1−C5−M around the metal-carbon bonds in the M-C5 ring (Scheme 1) as a metric for quantifying the degree of geometric bending in metallabenzenes. A deviation of α from 180° serves as an indicator of non-planarity. To probe their aromaticity, we assembled a dataset comprising 127 bent metallabenzenes, 69 Osmabenzene, 38 Ruthenabenzene, and 20 Iridabenzene complexes (refer to Figs. S1-S5 in Supporting information for details). We utilized four theoretical indices [24,25] to assess the aromaticity: NICS values [26–32], ACID plots [33–35], GIMIC-derived net ring current strength [36–38], and EDDB for the total population of delocalized electrons [39–41]. Benzene was also analyzed for comparative purposes.

The NICS(1)$_{zz}$ indices calculated for the test dataset, as delineated in Figs. S1-S5, reveal a range of values from −0.07 to −15.63 for bent metallabenzenes. These values correspond to dihedral angles spanning from 142° to 175°, thereby substantiating the inherent aromaticity of these bent metallabenzenes, albeit to a lesser extent than benzene with the NICS(1)$_{zz}$ values. The GIMIC calculations yielded corroborative results, affirming the aromatic character of the metallabenzene complexes. Specifically, the induced ring current strength in benzene is approximately 12.00 nA/T, while it is observed to be below 8.00 nA/T for metallabenzenes, signifying a relative diminution in aromaticity. Notably, the GIMIC results align with the NICS data, reinforcing the aromatic nature of bent metallabenzenes.

The ACID isosurfaces, as depicted in Fig. S6 (Supporting information), demonstrate that the external diatropic component predominates over the internal paratropic component within the ring structure, thereby yielding a net diatropic current for both benzene and metallabenzenes, albeit with differing degrees of aromatic intensity. This observation aligns with the inferences made from NICS and GIMIC analyses (Tables S2-S14 and S15-S40 in Supporting information). Utilizing EDDB as an innovative metric for aromaticity, we characterize the extent of electron delocalization in these conjugated systems. Positive EDDB_F(r) values, as listed

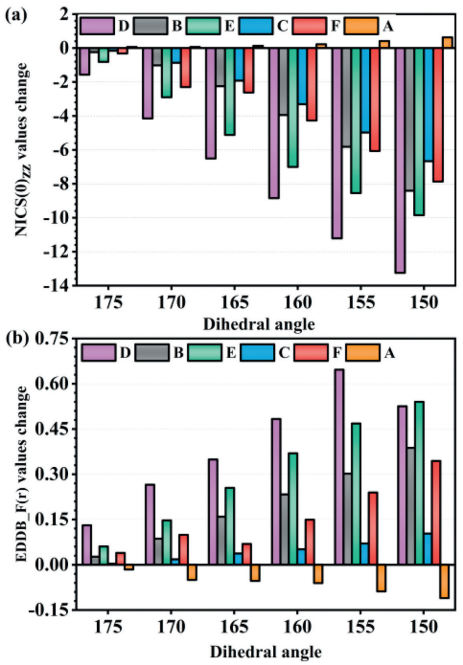

Fig. 1. The change of (a) the total NICS(0)$_{zz}$ values and (b) the EDDB_F(r) values of bent metalla-aromatics was displayed in comparison to their planar counterparts against the dihedral angle α ranging from 175° to 150°, as well as benzene.

in Tables S41-S44 (Supporting information), substantiate the aromatic character of metallabenzenes. The total population of delocalized electrons in these complexes is observed to range between 3.0 e and 5.0 e, which, although significant, remains below the corresponding value for benzene, approximately 5.6 e. In concordance with expectations, all four theoretical indices employed in this study collectively affirm the aromatic attributes of bent metallabenzenes, albeit to a degree that is somewhat attenuated in comparison to benzene.

Building upon our prior investigation, which employed NICS(1)$_{zz}$ values for a limited set of metallabenzene compounds, we have corroborated the aromatic nature of bent metallabenzenes using an expanded dataset and more rigorous methodology. Intriguingly, we observe that the aromaticity of metallabenzenes increases concomitantly with geometric bending. This unique property is substantiated by NICS, GIMIC, and EDDB_F(r) analyses, which collectively indicate an enhancement in aromaticity as the geometry deviates from planarity. In stark contrast, benzene, a prototypical planar aromatic compound, experiences a loss in aromaticity upon bending, as evidenced by the indices above.

As delineated in Scheme 2 and Fig. 1, the calculated NICS(0)$_{zz}$ values for metallabenzene complexes exhibit an increasingly negative trend as the dihedral angle varies from 180.0° to 150.0°. This is in stark contrast to benzene, which demonstrates an opposing behavior. To mitigate the influence of localized currents surrounding

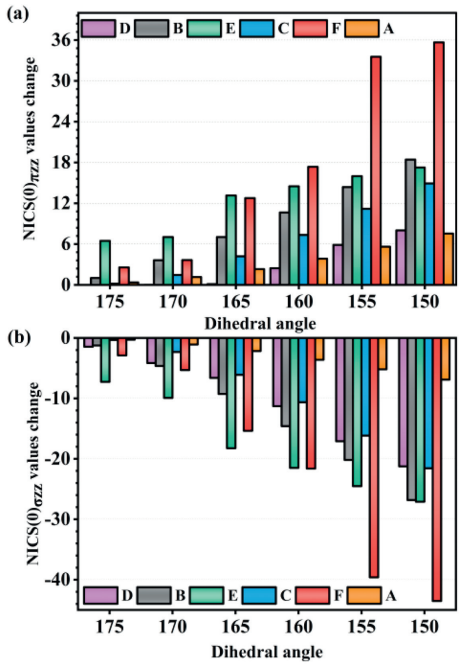

Fig. 2. The change of the NICS(0)π_{zz} (a) and NICS(0)σ_{zz} (b) values of bent metallaaromatics were displayed in comparison to their planar counterparts against the dihedral angle α ranging from 175° to 150°, as well as benzene.

the transition metal atoms and associated ligands, we performed calculations for the EDDB_F(r) values within the M-C5 ring. These findings are by the conclusions derived from both NICS and EDDB analyses, substantiating that non-planarity enhances the total population of delocalized electrons in metallabenzenes while concurrently reducing it in benzene. Furthermore, the calculated net ring current strength, measured in nA/T across the C2-C3 bonds in Fig. S7 (Supporting information), exhibits an augmentation rather than a diminution as the dihedral angle α deviates from 180.0° and approaches 150.0°.

We further explore the correlation between geometric bending and variations in the C-M bond length as well as the C-M-C angle in metallabenzenes. We employed osmabenzenes with diverse ligand configurations: Equatorial PH_3 and axial CO ligands (Fig. S8 in Supporting information), equatorial PH_3 and axial NH_3 ligands (Fig. S9 in Supporting information), and PH_3 ligands at both equatorial and axial positions (Fig. S10 in Supporting information) as representative models. Our analyses indicate that the degree of geometric bending increases with the shortening of the C-M bond length. Moreover, an increase in the C-M-C angle further accentuates geometric bending. These structural modifications lead to an elevation in distortion energy and enhanced aromaticity, corroborating the augmented aromaticity change we have observed.

Understanding the origins of their unique aromatic properties is imperative to unravel the enigmatic aromaticity of metallaaromatics and distinguishing them from traditional benzene-like aromatics. Beyond the contributions from the π-space orbitals, we also consider the significant role of the σ-space orbitals. Accordingly, we have analyzed and categorized the contributions of each canonical molecular orbital (CMO) [42–44] into the π- and σ-spaces (Fig. 2). Utilizing the most refined index, NICS(0)$_{zz}$, we eliminate contamination by dissecting the zz component of the tensor into its CMO contributions, denoted as NICS(0)π_{zz} and NICS(0)σ_{zz}, to quantify the respective contributions from the π and σ orbitals (refer to Tables S2-S14 for details).

Fig. 2 delineates that both the NICS(0)π_{zz} values for benzene and metallabenzenes escalate with increasing geometric bending, suggesting a concomitant decrease in aromaticity solely attributable to π orbital contributions for both systems. Conversely, the NICS(0)σ_{zz} values diminish with geometric bending, signifying an enhancement in aromaticity due to the σ orbital contributions. This reveals a congruent trend in aromaticity changes for both the π and σ orbitals in benzene and metallabenzenes, highlighting some commonality between traditional and metalla-aromatics. The ACID method was also utilized to segregate the overall contributions into the π- and σ-spaces (Figs. S11 and S12 in Supporting information). Contributions from the total π orbitals yield a net diatropic current, while those from the σ orbitals induce a paratropic ring current. In conjunction with the NICS indices, it can be inferred that the antiaromatic contributions from the σ orbitals are attenuated, and the aromatic contributions from the π orbitals are likewise diminished as the geometry deviates from planarity.

However, a salient distinction exists between benzene and metallabenzenes regarding the magnitude of the σ orbital contributions. Fig. 2 reveals that the σ orbitals overwhelmingly dictate the changes in aromatic properties upon geometric bending in metallabenzenes. In stark contrast, the π orbitals predominantly influence the aromaticity in benzene. Exhaustive theoretical studies have been carried out to investigate the impact of orbital interactions in both the π- and σ-spaces to determine which orbital exerts a significant influence on the aromaticity of metallabenzenes during geometric bending.

Fig. 3 contrasts the orbital interactions in metallabenzene with those in benzene. As depicted in Fig. 3a, the metal d_{xz} orbital is isolobal to the carbon p_z orbital, significantly contributing to the formation of benzene-like π orbitals. In addition, two metal d orbitals (d_{yz} and $d_{x^2-y^2}$) are identified that do not directly participate in this process, which we have termed 'extra orbitals'. Owing to symmetry considerations and the interactions between the metal d_{yz} orbital and the benzene-like π orbitals, the π-space orbitals of metallabenzene arise from these interactions (Fig. 3b). Further, by referencing our previous work on the σ orbitals of benzene [21], we demonstrate that the σ-space orbitals for metallabenzenes are generated through the interaction between isolobal benzene-like σ orbitals and the symmetry-adapted metal $d_{x^2-y^2}$ orbital (Fig. 3c). Consequently, the highest occupied molecular orbital in the π-space (π_{HOMO}) displays an antibonding character between the metal fragment and the C5 ring. Similarly, the $d_{x^2-y^2}$ orbital can be considered an additional σ orbital compared to benzene, leading to the emergence of another highest occupied molecular orbital in the σ-space (σ_{HOMO}) that exhibits antibonding character.

As illustrated in Fig. 4, there is a gradual increase in the values of the σ_{HOMO}, π_{HOMO}, and σ_{HOMO-1} orbital. The total variable quantity of CMO-NICS values in both σ_{HOMO} and π_{HOMO} orbitals is below 4.0 as the dihedral angle transitions from 180° to 150°. As noted, the σ_{HOMO} and π_{HOMO} orbitals are tied up with the extra d_{yz} and $d_{x^2-y^2}$ orbitals in metallabenzenes. The observed change in the NICS values does not exhibit a significant deviation from the anticipated outcome. Nevertheless, the overall change in the σ_{HOMO-1} orbital, a molecular orbital resembling the σ_{HOMO} in benzene, shows a substantial increase of around 18.0, representing a fourfold increment compared to the previous value. These findings indicate only a slight effect of the σ_{HOMO} and π_{HOMO} orbital on the aromatic properties when the geometry undergoes distortion.

Additionally, it is evident from the data shown in Tables S45 and S46 (Supporting information) that the σ_{HOMO-1} orbital in illustrative metallabenzene complexes (B-F) all exhibit a significant increase in percentage as they undergo gradual bending. The contribution of the σ_{HOMO-1} orbital is unaffected by either the substitution of the axial ligands from B to C, the modification of the equatorial ligands from C to D, or the change in the type of transition atom. The σ_{HOMO-1} orbital of metallabenzene complexes emerge as the primary contributor to the change of aromatic properties with

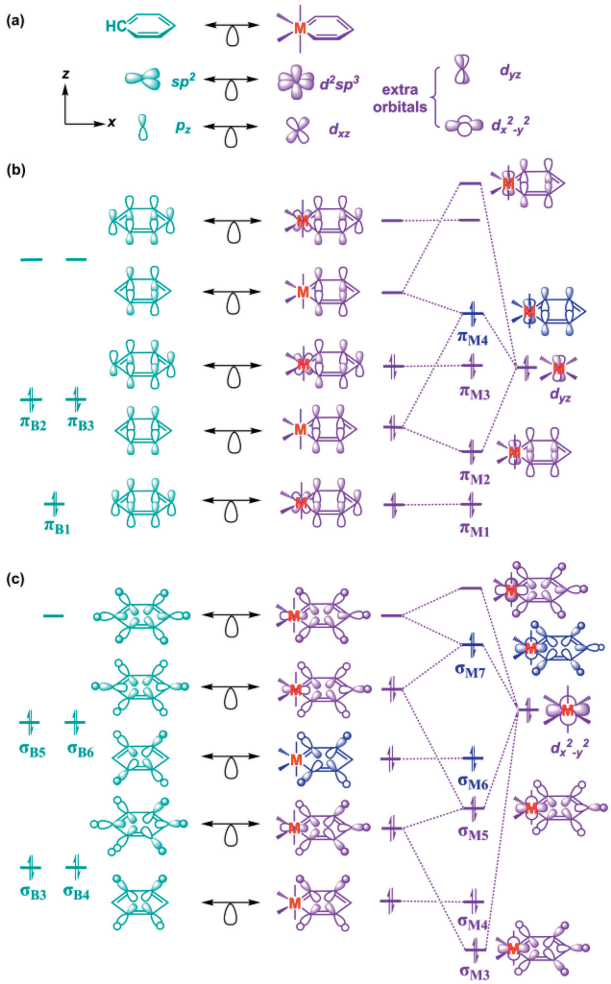

Fig. 3. (a) Isolobal analogy between benzene and metallabenzene in forming the C6 and MC5 rings, respectively. (b) π molecular orbitals of benzene and metallabenzene. (c) σ molecular orbitals of benzene and metallabenzene.

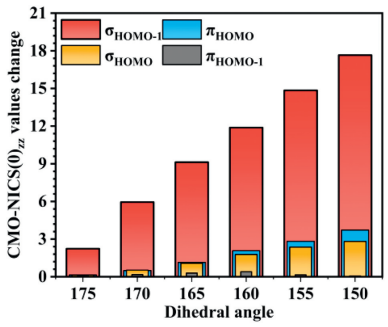

Fig. 4. The change of the NICS(0)$_{zz}$ values in some selected canonical molecular orbitals (CMOs) based on NBO program in metallabenzene complex C against the dihedral angle α ranging from 175° to 150°.

geometric bending, and its effect surpasses that of both the σ_{HOMO} and π_{HOMO} orbitals. It is noteworthy to acknowledge that the total change of the σ_{HOMO} in benzene should not be disregarded in Table S45. However, the aromaticity of benzene diminishes as the dihedral angle bends.

The contributions of selected benzene and metallabenzenes' orbitals are elaborated upon in Table S47 (Supporting information). The contribution ratio of the σ_{HOMO} orbital in benzene is notably high, reaching 32.17%. Concurrently, the cumulative effect within the π-space, accounting for as much as 41.88%, should not be overlooked. In contrast, Fig. 4 reveals that the total contribution ratio in the σ-space for metallabenzene escalates to an astonishing, significantly surpassing its π-space counterpart. Surprisingly, the σ_{HOMO-1} orbital, which is analogous to the HOMO orbital in benzene's σ-space, contributes as much as 38.78%, thereby achieving a position of preeminence. Both the σ_{HOMO} orbital in benzene and the σ_{HOMO-1} orbital in metallabenzenes exhibit a marked increase in their respective percentages as the dihedral angle narrows to 150°. Contrarily, the aromatic character manifests an inverse relationship. Meanwhile, the contribution ratio of each orbital in respective space are calculated in Tables S48-S53 (Supporting information), the σ_{HOMO-1} orbital realizes the exceed change, contributes as much as 66.28% in the total contribution of the σ-space. The underlying hypothesis for this counterintuitive observation posits that the σ-space, particularly the σ_{HOMO-1} orbital, substantially amplifies the aromaticity of metallabenzenes. While the σ-space in benzene does exert some influence on its aromatic character, this effect is marginally inferior to the overall contribution from the π-space.

Compared to benzene, comprehensive theoretical studies employing metallabenzene complex C (Scheme 2) as a representative model are presented in Figs. S13 and S14 (Supporting information). These studies reveal that the HOMOs in both the π- and σ-spaces remain relatively invariant. However, the σ_{HOMO-1} orbital, which is isolobal with benzene's σ_{HOMO}, undergoes a substantial shift in its aromatic properties. Intriguingly, the energy of the σ_{HOMO-1} orbital in metallabenzene complex C elevates from $E = -10.90$ eV to -10.65 eV as it transitions from a planar to a nonplanar conformation. Moreover, as the dihedral angle reaches 150°, the σ_{HOMO-1} orbital in bent metallabenzene complex C arises from interactions between the benzene-like σ orbital and the metal's d_{yz} orbital. In contrast, the σ_{HOMO-1} orbital in planar metallabenzene is constituted by interactions between the benzene-like σ orbital and the metal's d_{xy} orbital. The influence of structural bending necessitates the inevitable mixing of the σ and π orbitals. In order to objectively assess the degree of σ/π orbital mixing in the nonplanar complex, orbital projection calculations are performed in Tables S54-S58 (Supporting information). The weight of HOMO in π- and σ-space defined in the planar structure are both over 80% in the nonplanar structure while the weight of HOMO-1 in the σ-space in the planar structure has been as low as 52% in the nonplanar structure, which indicates a noticeable blending of the π orbitals. However, the orbitals in both the π- and σ-spaces of distorted benzene exhibit only minor deviations as can be seen in Table S5 (Supporting information). The disparity in aromatic character between the two complexes can be attributed to the incorporation of the metal atom. The aforementioned orbital interactions in the representative metallabenzenes are vividly illustrated in Fig. S15 (Supporting information) as they undergo geometric bending.

These observations provide compelling evidence in support of CMO–NICS analyses and orbital interactions. Bent benzene shows no significant changes in its orbitals and retains its aromaticity primarily through p_π-p_π conjugation. However, the bending of the dihedral angle adversely impacts benzene's aromatic nature. In stark contrast, the unique characteristics of transition-metal orbitals allow metallabenzenes to adopt nonplanar geometries while preserving their aromaticity. The sudden emergence of an additional d_{yz} orbital in the σ_{HOMO-1} orbital significantly enhances the aromaticity of bent metallabenzenes, leading to outcomes opposed to those observed in benzene.

In previous studies, we introduced the σ-control mechanism to elucidate the unexpected geometric distortion observed in metallabenzenes [21]. This concept was later extended to analyze the structural characteristics of both fused-ring metallabenzenes

[22] and heterometallabenzenes [23]. More recently, the scope of the σ-control mechanism has been broadened to explain the counterintuitive aromatic properties observed in metallabenzenes, moving beyond their mere structural features. Exploring this concept across a wider array of metalla-aromatic systems represents a compelling and significant avenue for future research. Currently, we have examined metallabenzene models with some first transition metal atoms as centers (Cr, Mn, and Fe) in Fig. S16 (Supporting information), despite the scarce experimental reports available on metallabenzene synthesis using these first transition metal centers. Our investigations have identified decreased aromaticity associated with geometric bending in metallabenzenes that feature first transition metal centers. Additionally, our studies indicate that the aromaticity of metallabenzenes with first transition metal centers are predominantly influenced by the π orbitals, diverging from those with second and third transition metal centers and aligning more closely with the behavior of benzene (Figs. S17–S19 in Supporting information). This divergence is tentatively attributed to the more contracted d orbitals of the first transition metals, diminishing the impact of metal d orbitals on the frontier orbitals. Given the importance of expanding the σ-control mechanism to other metalla-aromatic systems, we plan to undertake a comprehensive investigation of the structural and aromatic characteristics of metallabenzenes with first transition metal centers, along with isolobal fused-ring metallabenzenes and heterometallabenzenes.

In summary, we have systematically explored the intriguing aromaticity of bent metallabenzenes. Our computational analyses reveal that these bent metallabenzenes exhibit unique aromatic characteristics, albeit to a lesser extent than benzene. Incorporating a metal fragment imbues metallabenzenes with exceptional properties, primarily due to the involvement of d orbitals. Notably, their aromaticity is amplified upon significant geometric bending, starkly contrasting to benzene, which experiences diminished aromaticity as it deviates from planarity. Contributions from π-space orbitals attenuate the aromatic features in both benzene and metallabenzenes upon bending. Conversely, the σ-space orbital contributions enhance aromaticity as the molecules transition from planar to non-planar geometries. Rigorous theoretical investigations pinpoint the predominance of the $\sigma_{\mathrm{HOMO-1}}$ orbital in metallabenzenes, which corresponds to benzene's HOMO orbital in the σ-space. This underscores the necessity of focusing on the σ-space orbitals when investigating metalla-aromatics, which diverge significantly from traditional aromatic systems. Consequently, the applicability of our proposed σ-control mechanism is broadened, through the further integration of precise computational approaches [45–48], highlighting its potential in guiding the rational design of functional metalla-aromatic materials [49–54].

Declaration of competing interest

The authors declare that they have no known competing financial interests or personal relationships that could have appeared to influence the work reported in this paper.

Acknowledgment

This work was supported by the National Natural Science Foundation of China (Nos. 22173105, 22173104, 21973094).

Supplementary materials

Supplementary material associated with this article can be found, in the online version, at doi:10.1016/j.cclet.2024.109770.

References

[1] B.E. Bursten, R.F. Fenske, Inorg. Chem. 18 (1979) 1760–1765.
[2] P.V. Schleyer, Chem. Rev. 101 (2001) 1115–1117.
[3] H.J. Wang, X.X. Zhou, H.P. Xia, Chin. J. Chem. 36 (2018) 93–105.
[4] B.J. Frogley, L.J. Wright, Chem. Eur. J. 24 (2018) 2025–2038.
[5] D.F. Chen, Y.H. Hua, H.P. Xia, Chem. Rev. 120 (2020) 12994–13086.
[6] B.R. Cuyacot, Z. Badri, A. Ghosh, C. Foroutan-Nejad, Phys. Chem. Chem. Phys. 24 (2022) 27957–27963.
[7] M. Luo, D.F. Chen, Q. Li, H.P. Xia, Acc. Chem. Res. 56 (2023) 924–937.
[8] J.R. Bleeke, Chem. Rev. 101 (2001) 1205–1227.
[9] J.R. Bleeke, Acc. Chem. Res. 24 (1991) 271–277.
[10] L.J. Wright, Dalton Trans. 15 (2006) 1821–1827.
[11] C.W. Landorf, M.M. Haley, Angew. Chem. Int. Ed. 45 (2006) 3914–3936.
[12] J. Chen, G. Jia, Coord. Chem. Rev. 257 (2013) 2491–2521.
[13] W. Wei, X. Xu, H.H.Y. Sung, I.D. Williams, Z. Lin, G. Jia, Angew. Chem. Int. Ed. 61 (2022) e202202886.
[14] D.L. Thorn, R. Hoffmann, New J. Chim. 3 (1979) 39–45.
[15] I. Fernandez, G. Frenking, Chem. Eur. J. 13 (2007) 5873–5884.
[16] I. Fernandez, G. Frenking, G. Merino, Chem. Soc. Rev. 44 (2015) 6452–6463.
[17] W.Y. Hung, J. Zhu, T.B. Wen, et al., J. Am. Chem. Soc. 128 (2006) 13742–13752.
[18] M. Tauqeer, R.S. Ji, A.K. Singh, et al., Eur. J. Inorg. Chem. 2018 (2018) 3126–3130.
[19] C. Yu, M. Zhong, Y. Zhang, et al., Angew. Chem. Int. Ed. 59 (2020) 19048–19053.
[20] J. Zhu, G.C. Jia, Z.Y. Lin, Organometallics 26 (2007) 1986–1995.
[21] Z.N. Chen, G. Fu, I.Y. Zhang, X. Xu, Inorg. Chem. 57 (2018) 9205–9214.
[22] X. Jia, Q. Zhou, J. Chen, L. Zhang, Z.N. Chen, J. Phys. Chem. A 124 (2020) 7071–7079.
[23] X. Qin, Q. Zhou, Z.N. Chen, L. Zhang, Organometallics 42 (2023) 2148–2158.
[24] R. Gershoni-Poranne, A. Stanger, Chem. Soc. Rev. 44 (2015) 6597–6615.
[25] M. Homray, A. Misra, P.K. Chattaraj, Curr. Org. Chem. 21 (2017) 2699–2704.
[26] P.V. Schleyer, C. Maerker, A. Dransfeld, H.J. Jiao, N. Hommes, J. Am. Chem. Soc. 118 (1996) 6317–6318.
[27] Z.F. Chen, C.S. Wannere, C. Corminboeuf, R. Puchta, P.V. Schleyer, Chem. Rev. 105 (2005) 3842–3888.
[28] H. Fallah-Bagher-Shaidaei, C.S. Wannere, C. Corminboeuf, R. Puchta, P.V. Schleyer, Org. Lett. 8 (2006) 863–866.
[29] A. Stanger, Eur. J. Org. Chem. 2020 (2020) 3120–3127.
[30] S. Radenkovic, S. Dordevic, Phys. Chem. Chem. Phys. 23 (2021) 11240–11250.
[31] A. Stanger, ChemPhysChem 24 (2023) e202300080.
[32] M.D. Zermeno-Macias, M.M. Gonzalez-Chavez, F. Mendez, et al., Molecules 26 (2021) 5078.
[33] J. Gomes, R.B. Mallion, Chem. Rev. 101 (2001) 1349–1383.
[34] R. Herges, D. Geuenich, J. Phys. Chem. A 105 (2001) 3214–3220.
[35] D. Geuenich, K. Hess, F. Köhler, R. Herges, Chem. Rev. 105 (2005) 3758–3772.
[36] H. Fliegl, S. Taubert, O. Lehtonen, D. Sundholm, Phys. Chem. Chem. Phys. 13 (2011) 20500–20518.
[37] D. Du, D. Sundholm, H. Fliegl, J. Chin. Chem. Soc. 63 (2016) 93–100.
[38] M. Rauhalahti, D. Sundholm, M.P. Johansson, Phys. Chem. Chem. Phys. 23 (2021) 16629–16634.
[39] D.W. Szczepanik, M. Andrzejak, J. Dominikowska, et al., Phys. Chem. Chem. Phys. 19 (2017) 28970–28981.
[40] D.W. Szczepanik, Comput. Theor. Chem. 1100 (2017) 13–17.
[41] R.R. Aysin, S.S. Bukalov, Russ. Chem. Bull. 70 (2021) 706–714.
[42] T.C. Chang, J. Chin. Chem. Soc. 43 (1996) 1–5.
[43] E.D. Glendening, C.R. Landis, F. Weinhold, J. Comput. Chem. 40 (2019) 2234–2241.
[44] O.I.O.M. Abdelkarim, A. Asiri, Comput. Theor. Chem. 1210 (2022) 113637.
[45] Y. Zhang, X. Xu, W.A. Goddard, Proc. Natl. Acad. Sci. U. S. A. 106 (2009) 4963–4968.
[46] N.Q. Su, Z. Zhu, X. Xu, Proc. Natl. Acad. Sci. U. S. A. 115 (2018) 2287–2292.
[47] Y. Wang, Y. Li, J. Chen, I.Y. Zhang, X. Xu, JACS Au 1 (2021) 543–549.
[48] Z.N. Chen, T. Shen, Y. Wang, I.Y. Zhang, CCS Chem. 3 (2021) 136–143.
[49] S.Y. Chen, L.X. Peng, Y.N. Liu, et al., Proc. Natl. Acad. Sci. U. S. A. 119 (2022) e2203701119.
[50] X. He, F. Gan, Y. Zhou, et al., Small Methods 5 (2021) 13.
[51] S. Gupta, S. Su, Y. Zhang, et al., J. Am. Chem. Soc. 143 (2021) 7490–7500.
[52] Y. Zhang, C. Yu, Z. Huang, et al., Acc. Chem. Res. 54 (2021) 2323–2333.
[53] W.S. Wong, M. Stepien, Trends Chem. 4 (2022) 573–576.
[54] H.C. Liu, K. Ruan, K. Ma, et al., Nat. Commun. 14 (2023) 5583 -5583.